



## ABSOLUTE DATING OF ROCK ART ON FLAT MARBLE SURFACES

PAOLO EMILIO BAGNOLI\*

### ABSTRACT

*The present paper deals with the computer-aided simulation of the erosion processes on a flat marble limestone surface with ancient rock engravings. The main goal is to demonstrate that the engravings are still visible after a long time exposure to natural erosion. The mathematical technique used is the so-called Montecarlo method which consists of the study of the macroscopic properties of a granular system starting from the continuous repetition of microscopic stochastic events whose probability laws is supposed to be known. These laws were related to the speeds of the various erosion mechanisms for limestone. By using the above described procedure, it was possible to observe the time evolution of the cross-section of the engravings in a time range spanning about 2000 years and to evaluate the trend behaviours of both depth and width of the small moat. From the analysis of these trends, a method for absolute dating of the engravings was obtained. In the last part of the present paper, the results of the first experimental application of the present method on the so-called "Billhook Step" (Mount Gabberi, Camaione, Lucca) are exposed and discussed.*

### RIASSUNTO

Il presente articolo tratta della simulazione al computer dei processi di erosione di una superficie orizzontale di marmo carbonatico su cui sono presenti delle incisioni. Lo scopo è quello di dimostrare che i segni incisi nella roccia sono osservabili anche dopo un lungo tempo di erosione. La tecnica matematica usata è il cosiddetto metodo Montecarlo. Esso consiste nella ripetizione di un gran numero di eventi completamente casuali, di cui si suppone nota la legge di probabilità in funzione delle velocità dei vari processi erosivi, corrispondenti al distacco di piccole quantità elementari di materia ed in relazione al numero dei legami di connessione con il substrato roccioso. Questo procedimento consente di osservare nel tempo l'evoluzione della sezione di solchi incisi effettuati fino a 2000 anni fa e di misurare i parametri matematici che regolano l'evoluzione della larghezza e della profondità del solco. Dai rapporti che legano tali parametri e dalla conoscenza dei valori odierni delle due dimensioni, è stato possibile ottenere una formula per calcolare il tempo intercorso dall'esecuzione dell'incisione e quindi una datazione assoluta. Infine vengono riportati e discussi i primi risultati di misure sperimentali effettuate sul campo sul sito denominato Ripiano dei Pennati sul versante occidentale del Monte Gabberi (Camaione, Lucca).

### RESUME

*Cet article traite de la simulation à l'ordinateur des processus d'érosion sur une surface plane calcaire en marbre avec des anciennes gravures rupestres. Le but principal est de montrer que les gravures sont encore visibles après une longue exposition à l'érosion naturelle. La technique mathématique utilisée est ladite méthode Monte-Carlo qui consiste en l'étude des propriétés macroscopiques du système granulaire à commencer par la répétition continue des événements microscopiques stochastiques desquels on pense connaître les lois de probabilité. Ces lois sont en relation avec les vitesses des différents mécanismes d'érosion du calcaire. En utilisant la procédure ici décrite, il était possible d'observer l'évolution temporelle des échantillons de gravures dans un laps de temps de 2000 ans et d'évaluer les tendances évolutives de la profondeur et de la largeur du petit fossé. A partir de l'analyse de ces tendances, on a obtenu une méthode pour la datation absolue des gravures. Dans la partie finale de cet article, les résultats de la première application expérimentale de cette méthode sur ledit « Ripiano dei Pennati » (Mont Gabberi, Camaione, Lucca), sont exposés et traités.*

---

\* Paolo Emilio Bagnoli

Department of Information Engineering, University of Pisa, via Caruso 16, 56100 Pisa, Italy  
Phone: +39 050 2217511, Fax: +39 050 2217522, Email: p.bagnoli@iet.unipi.it

## INTRODUCTION

In a previous work [Bagnoli, P.E., Panicucci, N., Viegi, M., 2005], presented at the Conference Ante et Post Lunam II focused on the archaeology of the Apuane Alps and organized by the Apuanian National Park, the main characteristics of the figurative rock art within the mountains were exposed and discussed. These rock art sites show the figures of billhooks (Italian “pennato” or “roncola”), the curved hand-blades of the wood cutters, as the most occurring subject, mainly localized on horizontal flat marble surfaces at high and overlooking positions.

In the same work it was clearly exposed how the chronology of these figures, which are realized in contour line only, in real scale and showing an extreme degree of consumption, is extremely difficult because of the lack of comparisons with other sites elsewhere in Italy, except for two billhooks representations in the southern part of Trentino ( Riva del Garda and Arco).

In the local literature different and opposite hypotheses can be found concerning the interpretation and the chronology of these figures: from the Celtic-Etruscan age, the Roman period, related to the Silvanus god cult [Citton, G., Pastorelli, I., 1995], [Citton, G., Pastorelli, I., 2001], [Sani G., 2006], to the generic relationship with a “sheepers” culture [Guidi O., 1992], until the assigning to the modern age since some people retain that ancient figures cannot be preserved for a long time on limestone.

The present research started just from the above chronological problem: from the analysis of the stone erosion processes on the limestone of the Apuane Alps and of the evolution in time of the cross-section of an engraved sign, it tries to add further objective data to the discussion about the origin and the meaning of these artefacts.

The time evolution of an engraved small moat was studied with the help of computer simulations using the so-called Montecarlo method. This mathematical simulation technique allows obtaining information on the macroscopic characteristics of a granular system (i.e. composed by a very large number of microscopic elements) starting from the continuous repetition of stochastic events at microscopic scale, as for instance the removal of small marble particles, whose probability laws are supposed to be known.

Using the above described method, which needs as input data the average erosion speeds due to the natural physical-chemical erosion processes of the marble (in particular the freeze-thaw cycles and the chemical dissolution of calcium-carbonate into soluble calcium-bicarbonate) and overall of the average annual rain fall, it was possible to obtain the time evolution of an engraved small moat profile in the range 0 - 2000 years and therefore to accurately characterize the trend mathematical behaviours with which the two main dimensions of the moat, width and depth, change in time.

As it will be shown later, from the knowledge of the trend laws and using accurate experimental measurements of the modern values of the sign dimensions, it was possible to built an algorithm able to yield the time elapsed from the sign execution and therefore an absolute dating for the rock art. In the followings the simulation procedure is explained in all the details and the results of a first application of the present method on one of the most important Apuanian rock art site, the “Billhook step” (Il “Ripiano dei Pennati”, mount Gabberi, Camaiore, western side of the Apuane Alps), is extensively exposed and discussed.

## THE SIMULATION PROCEDURE

The marble block, to which the simulation procedure was applied and whose structure is depicted in Figure 1, is composed by a regular net of elementary cubic cells representing the smallest material clusters subjected to erosion. Since the lateral dimensions ( $L_x, L_y=15$  cm) of the block can be arbitrarily chosen, the single cell size depends upon the number of cells ( $n_x, n_y, n_z$ ) along the  $x, y$  and  $z$  directions. The horizontal top surface of the block is exposed to the upper environment, while the bottom one must be considered as unlimited. On the lateral sides along the  $x$  and  $y$  directions cylindrical-like boundary conditions exist. It means that, being  $x_i, y_i$  and  $z_i$  the coordinates of the centres, the cells placed on the lateral faces having  $x_i=1$  or  $x_i=n_x$  may be considered in contact with those on the opposite face and having the  $x$  coordinates  $x_i=n_x$  or  $x_i=1$  respectively. On the top surface of the block a parabolic-shaped linear small moat was engraved along the  $y$  direction in the centre of the  $x$  side. This particular geometry chosen, together with the cylindrical boundary conditions in the  $y$  direction and since the erosion mechanisms may be retained as uniform along  $y$ , allow us to decrease as much as possible the number of cells in the  $y$  direction in order to minimize the calculation time needed for the simulation procedure ( $n_x=1000; n_y=5$ ).



In a regular cubic network each cell is directly bound to 26 surrounding cells, including those in the diagonal directions. If a cell has all the 26 surrounding boundaries occupied, it means that this cell is located within the bulk of the material. If some of the boundary cells lack, it implies that the given cell is located close to the top surface.

The above defined solid may be described, from the mathematical point of view, by a couple of three-dimensional matrices in which the three indices  $ix$ ,  $iy$  and  $iz$  of the elements indicate the position of the cells in the three-dimensional space. In the first binary matrix, named AL (alive), the elements assume the values true, if the corresponding cell is still connected to the solid, or false if it has been previously eroded away. The second integer matrix, named FB (free boundaries) contains the number of unbounded boundaries for each cell.

The simulation of the marble erosion process as a function of time was carried out under the assumption of the following hypotheses. A) The original top surface of the rock is perfectly horizontal. B) Only the two above cited erosion mechanisms were taken into account. This implies that any other source of rock deformation, such as mechanical abrasions due to ice motion, is excluded. C) The intensity of the erosion mechanisms is uniform along the whole top surface of the sample block.

The simulation procedure is divided into 2000 time steps: the duration of one step was conventionally set to one year. Furthermore within a single time step the two erosion processes, simultaneously occurring in the reality, were applied in sequence: the first one is due to the freeze-thaw cycles while the second one is due to the chemical dissolution of calcium carbonate. The sequential application of the two processes instead of simultaneous can be a reasonable approximation and implies a great simplification of the simulation procedure.

The simulation of the surface erosion was implemented using the following method. Two probability distributions  $P_a(\text{FB})$  and  $P_b(\text{FB})$  were defined as a function of the number of the free boundaries of the cells and for the two erosion processes respectively. Both the functions  $P_a$  and  $P_b$ , which are increasing with the FB values, must be chosen with the following properties:

$$\begin{aligned} P(\text{FB}) = 0 & \quad \text{for} \quad \text{FB} = 0 \\ 0 < P(\text{FB}) < 1 & \quad \text{for} \quad 0 < \text{FB} < 26 \\ P(\text{FB}) = 1 & \quad \text{for} \quad \text{FB} = 26 \end{aligned} \tag{1}$$

In a single time step, for each 'alive' cell close to the top surface, i.e. having the corresponding  $AL(ix, iy, iz)$  value true and the  $FB(ix, iy, iz)$  value greater than zero, the computer generates a random number  $S$  in the range 0-1 using a uniform stochastic distribution. The removal or not of the cell is ruled by the following conditions:

$$\begin{aligned} S \leq P[FB(ix, iy, iz)] & \rightarrow AL(ix, iy, iz) = 0 \\ S > P[FB(ix, iy, iz)] & \rightarrow AL(ix, iy, iz) = 1 \end{aligned} \tag{2}$$

After that the erosion in the single time step is completed, both the matrices AL and FB are updated. The probability function  $P_a$  for the freeze-thaw erosion process was defined as follows:

$$P_a(\text{FB}) = \left(\frac{\text{FB}}{26}\right)^\alpha; \quad 0 < \alpha < \infty; \tag{3}$$

where the exponent  $\alpha$  decides the concavity of the curve: upward if  $\alpha > 1$  and downward if  $\alpha < 1$ . Figure 2a shows the probability distribution  $P_a$  as a function of the number of free boundaries FB and for several values of the exponent  $\alpha$ . Note that this parameter is directly related to the average erosion rate  $V_a'$  (measured in cell/step), so that the amount of the eroded material in a single time step can be finely modulated by changing the parameter  $\alpha$  in the probability function. The dependence of the erosion speed on the exponent is shown in the Figure 2b. This curve was calculated from many simulation tests performed on a small size flat marble block using only the  $P_a$  function with several values of its exponent.

The shape of the second probability function  $P_b$  for the calcium-carbonate dissolution process was defined starting from the inverse of the well-known Fermi-Dirac function, ruling the energy

electron probability occupation in a semiconductor crystal. Pb can be calculated from the following function normalized at FB=0 and FB=26 in order to exactly satisfy the rules defined in equation (1):

$$f(FB) = 1 - \frac{1}{1 + \exp\left[\frac{\beta(FB - FBo)}{26}\right]} \quad (4)$$

The above function has two different parameters: b and FBo. The first one (b) rules the shape of the curve from a sharp vertical step (for  $\beta \rightarrow \infty$ ) to a line (for  $\beta \rightarrow 0$ ). The second parameter FBo can be defined as the number of free boundaries for which  $f(FBo)=0.5$ . The so-built Pb function is shown in Figure 2c as a function of the free boundaries FB, for  $b = 12$  and for several values of the parameter FBo. Also in this case, the average erosion speed due to the calcium-carbonate dissolution process  $Vb'$  (measured in cells/step) is directly related to the shape of the Pb curve and in particular to the FBo value, as can be seen from the plots of Figure 2d. Here the parameter FBo is plotted as a function of the erosion speed  $Vb'$  (cells/step) for several values of the parameter b. Similarly these curves were calculated by performing several simulation tests on a small size flat marble block and using only the Pb distribution.

The parameters characterizing the two probability distribution functions, a for Pa and FBo for Pb, were chosen accordingly to the values of the average erosion speeds Va and Vb (measured in mm/year) found in literature for environmental conditions similar to those in which the rock under study is located. The corresponding velocities  $Va'$  and  $Vb'$  measured in cells/step can be simply obtained from the following relationships:

$$Va' = Va \cdot (nx/Lx) ; \quad Vb' = Vb \cdot (nx/Lx) \quad (5)$$

where the ratio  $Lx/nx$  is the lateral size of the cubic cells. The parameters of the two distribution functions were chosen from the plots of the Figures 2b and 2d respectively used as look-up tables.

#### Erosion speed correction factors

In the above description of the simulation procedure, the hypothesis C of the uniform intensity of both the erosion mechanisms implies that the speeds, and hence the probability distributions, should be always the same for all the exposed cells. This assumption may be quite unrealistic in the small scale dimensions since local morphological factors may concur to change the erosion conditions. Therefore in each time step the Va and Vb speeds - and consequently the parameters of the probability functions - must be changed using suitable correction functions depending on the depth of the cells within the engraved moat and on the local morphology of the exposed top surface.

In particular the erosion process due to freeze-thaw cycles may be considered as slightly more intense at the top surface of the engraved moat than at the bottom and the increase percentage must be referred to the original depth of the moat. This process may be described by a correction function  $Cza(iz)$  which depends only on the z spatial variable of the cells. Furthermore it must be emphasized that the borders of the moat are subjected to more intense freeze-thaw erosion than a flat surface. This second modification can be implemented by introducing a further correction function  $Cxa(ix)$  which depend only on the x spatial variable. However this implies that the program needs to recognize, after each simulation time step, the localization of the borders of the moat using a suitable numerical algorithm. Therefore for each cell the velocity Va, and consequently the  $Va'$  speed and the parameter a of the probability function Pa, must be corrected using the following relationship.

$$Va(ix, iy, iz) = Vao \cdot Cxa(ix) \cdot Cza(iz) , \quad (6)$$

where Vao is the standard value of the erosion speed. As an example, Figure 3a shows the cross section of the surface under simulation taken at a given time and the horizontal and vertical plots of the  $Cxa(ix)$  and  $Cza(iz)$  functions respectively. The maximum values for the two functions are open parameters of the simulation tests and in any case they do not exceed 20% of the standard value.

For the calcium-carbonate dissolution process, many works can be found in literature concerning theoretical and experimental studies of the erosion on limestone rock surfaces. In particular, the recently published study reported in the reference [Szunyogh 2005] deals with an accurate mathe-



mathematical model for carbonate-based rocks dissolution, which takes into account many environmental parameters, as the annual rainfall and the slope of the rock surface with respect to the horizontal plane. According with the above model and assuming a vertical rainfall, the surface lowering  $W$  speed can be written in a compact form as follows:

$$W = (g \cdot Q_a) / [u + Q_a \cdot \cos(\vartheta)] \quad (7)$$

$Q_a$  is the annual precipitation,  $\vartheta$  is the angle of the local slope of the surface with respect to the horizontal plane and the parameters  $g$  and  $u$  are defined by the following relationships:

$$g = (k \cdot C_{eq} / \rho_{rock}) \cdot t_d \cdot S_H \cdot N_a \cdot M_{mm} \quad (8)$$

$$u = k \cdot t_d \cdot S_H \cdot N_a \quad (9)$$

where  $k$  is the velocity constant of the chemical dissolution at 10 °C and in open-air carbon dioxide content,  $C_{eq}$  is the equilibrium concentration of calcium carbonate,  $\rho_{rock}$  is the density of stone,  $t_d$  is hours/day rainfall time and  $S_H$  (3600 sec/hour),  $N_a$  (365 days/year) and  $M_{mm}$  (1000 mm/m) are suitable constants applied to convert the parameter dimensions into those used in everyday practice. From equation (7) it can be clearly seen that the velocity  $W$  is a function of the local slope of the rock surface. Figure 3b shows the plots of the  $W$  speed versus the annual precipitation (assuming  $t_d = 10$  hours/day) for several values of the angle  $\vartheta$ , while in the Figure 3c the same plots are drawn normalized with respect to the curve with  $\vartheta = 0^\circ$ . On the basis of the above model it can be stated that the dissolution velocity on the sample under simulation, in each time step is a function of the local slope of the exposed surface. Therefore, notwithstanding that most of the original surface is nearly flat, the walls of the engraved moat undergo increased erosion with respect to the standard situation. Once that a suitable value for the annual precipitation has been set, at the end of each simulation time step the local slope can be calculated from the absolute value of the surface profile first derivative along the  $x$  axis. Of course, in order to eliminate the effects of the surface roughness on the derivative function, the surface profile is previously smoothed using a mobile averaging filtering procedure. These data, interpolated within the plots of the Figures 3b and 3c, allow us to calculate the horizontal correction function  $C_{xb}(ix)$  for the velocity  $V_b$ .

The corresponding vertical correction function  $C_{zb}(iz)$  for the dissolution process may be built in a similar way than that for the freeze-thaw cycles but in this case, due to the accumulation of water, the standard value is located at the upper surface while at the bottom of the engraving the erosion velocity is higher. Therefore the local dissolution velocity  $V_b$ , can be similarly expressed by the following relationship:

$$V_b(i_x, i_y, i_z) = V_{bo} \cdot C_{xb}(i_x) \cdot C_{zb}(i_z) \quad (10)$$

where  $V_{bo}$  is the standard value calculated for  $\vartheta = 0^\circ$ .

#### SIMULATION RESULTS

The values of the rock dissolutions rates for the two erosion processes were deduced from the data found in literature. In particular reference [Buhmann D. & Dreybrodt W. 1985] reported the average erosion thickness due to a single freeze-thaw cycle for several types of rock material. For carbonate limestone the value is about  $5.5 \times 10^{-5}$  mm. Using this value and considering as a first approximation one cycle per day during four month per year, we obtain an average value of 0.010038 mm/year for the erosion speed  $V_a$  corresponding to a  $V_a'$  value equal to 0.0669 cells/year in the present simulation model ( $L_x=150$  mm;  $n_x=1000$ ).

As far as the chemical dissolution rate is concerned, we used the data reported in reference [Szunogh 2005] for the involved physical parameters to calculate the equations (8) and (9). However, as shown in the equation (7), the most important input parameter needed by the simulation procedure is the average annual rain fall  $Q_a$ . In the lack of accurate scientific data concerning the local evolution of this parameter back to 2000 years and coming from geological analyses, the annual rain fall was provisionally deduced from the historical data of up to eleven meteorological measurement

stations located around the central massif of the Apuane Alps and at various different altitudes. The time range spanned by the data was about 80 years.

In the Figure 4 the  $Q_a$  values for the various stations are plotted as a function of the altitude; the dashed line represents the linear regression of the data set. The value used as the most probable one for the rock art site under investigation was interpolated along the regression line and was 2150 mm/year. Consequently the mean chemical dissolution velocity  $V_b$  for the horizontal condition ( $q = 0^\circ$ ) was calculated from equation (7) as 0.0459 mm/year corresponding to  $V_b' = 0.3066$  cells/year.

Using the above input parameters, several simulation runs were performed on various models in which the initial depth ( $h_0$ ) and width ( $w_0$ ) of the engraved parabolic moat varied in the following ranges:  $h_0 = 3 - 10$  mm and  $w_0 = 5 - 22.5$  mm.

The Figure 5 shows in isometric scales the rock surface cross-sections along the x-direction of two sample models drawn every 100 years. The small dots indicate the borders of the trace as detected by the internal algorithm. As can be seen from this figure, the engraved signs are still observable after long time erosion notwithstanding the progressive widening of the width, the smoothing of the borders and the lowering of the top surface.

From the results of the performed simulations a general trend in the evolution of the engraved trace profile may be achieved as shown by the plots of Figure 6a and 6b. In order to smooth the statistically induced roughness of the surface, in these figures each curve was obtained by averaging the plots of ten different simulations with the same parameters.

As can be clearly seen, the depth tends to slowly increase in time with a linear behaviour and the increasing speed ( $K_1$ ) was found to be independent on the original depth  $h_0$ . On the contrary the width evolves linearly with the square root of time, except in the initial range, and the slope ( $K_2$ ) and the intercept ( $w_0'$ ) are increasing functions of the original depth  $h_0$ . This behaviours can be practically described as a function of time  $t$  by means of the following set of equations:

$$h = h_0 + K_1 \cdot t \quad ; \quad w = w_0' + K_2 \cdot \sqrt{t} \quad (11a)$$

$$K_2 = a + b \cdot h_0 \quad ; \quad w_0' = c + d \cdot h_0 \quad (11b)$$

where the parameters  $a$ ,  $b$ ,  $c$  and  $d$  are constants which can be calculated from the plots of equations (11b) as a function of the initial depth  $h_0$  and shown in the Figure 6c. By replacing the square root of time with the variable  $x = t^{1/2}$  and knowing the today values of the engraving width  $w$  and depth  $h$ , the elapsed time from the engraving execution can be obtained from the positive real root of the following third order equation:

$$x^3 + \frac{d}{b} x^2 - \frac{a + b \cdot h}{b \cdot K_1} x + \frac{w - c - d \cdot h}{b \cdot K_1} = 0 \quad (12)$$

As a first application test of the above described algorithm, a self-dating procedure was applied to the two simulation curves shown in the Figure 5. For every time step (year) the obtained values for the height  $h$  and the width  $w$  were used as input data in the equation (12), while the trend parameters  $a$ ,  $b$ ,  $c$  and  $d$  were calculated from the averaging of several simulation tests performed using the same  $h_0$  and  $w_0$  parameters and the same average annual rain fall  $Q_a$ . The output value of the elapsed time was compared with the initial available value.

The Figure 7 shows the results of this procedure. Here the relative error percentage between the true elapsed time and the back calculated one using the dating algorithm was plotted as a function of time. As can be seen, the dating algorithm is able to estimate the antiquity of the engraving with a relative error in the range of 10-20%, at least under the above described conditions and overall using a single couple of data for  $h$  and  $w$ . This first result is quite encouraging for the rupestrian archaeology which mostly uses cultural and typological considerations for the chronological analyses.

However it must be pointed out that the curves of the Figure 7 are affected by a random error only, having zero mean value and caused by the granular nature of the phenomenon and which is responsible of the differences of the real deformation curves from the corresponding average trend behaviours. In order to increase the accuracy of the evaluation, at least from the random error point of view, we must apply the algorithm to several experimental measurement on the same sample (i.e.



several couples of  $h$  and  $w$  taken on the same engraved figure) and averaging the output values.

The second source of error, which does not affect the plots of the Figure 7, is the “systematic” one induced by an inaccurate evaluation of the main parameters ruling the erosion speed (as for instance the average annual rain fall) and causing always the same error on all the output data.

#### EXPERIMENT

The above described method was applied to the rock art site called the “Billhooks Step” (Italian “Ripiano dei Pennati”) on the western side of the Mount Gabberi (Camaiole, Lucca). This flat rock, located at an altitude of 960 meter above the sea level, on the top of a sharp cliff overlooking the sea coast, is one of the sites described in the reference [Bagnoli, P.E., Panicucci, N., Viegi, M., 2005] having such properties for which a high chronology may be assigned, following the criteria exposed in the same reference.

The complete map of the engraved rock is shown in the Figure 8. Here there are several figures of billhooks engraved around a small tub and three crosses, two having a Greek shape (four arms with the same length) and one belonging to the Latin type. The in situ experimental activity, which consisted of the measurements of several engraved profiles on some figures, were carried out by the author with the precious help of some volunteers belonging to the Archaeological and Speleological Group of Pietrasanta (GASP) and to the UOEI association of Pietrasanta who also provided the security equipments.

The dating method was applied to a set of engraved figures composed by five billhooks (P1-P5) and the three crosses (C1-C3); in the Figure 8 the chosen artefacts are traced in black lines and marked with the corresponding label.

The cross-sections of the engraved figures were captured using a mechanical profiler made of parallel steel needles with a diameter of 1 millimetre and photographed using a high resolution digital camera with a grid paper on the background (see Figure 9). The digital image was then uploaded within a vectorial graphical program, such as AutoCad, in order to easily measure both the height and the width with an estimated resolution of less than 100 microns.

For each figure under test, up to ten different profiles were taken just for averaging the data.

The obtained results are shown in the Table I in numerical form and also in the Figure 10 in the graphical one for an easier reading.

In the Table I the first columns indicate the elapsed time from the engraving execution obtained as the mean value of the ten different measurements; the second columns contain the standard deviations of the data while in the third columns the corresponding absolute date calculated with respect to the year of the measurement execution (2006).

In order to clearly demonstrate the sensitivity of the output results on the annual rain fall, in both the Table I and the Figure 10 the output data obtained for two other different  $Q_a$  values (1750 mm/year and 2450 mm/year) are also reported for comparison with those calculated using the most probable value (2150 mm/year) for  $Q_a$ .

From a careful analysis of the obtained results some important details must be particularly noted. At first and as it was expected, the dates are progressively more recent with the increasing of the average annual rain fall value just because the higher speed of the chemical dissolution which, at least at the altitude considered, is largely predominant with respect of the effects of the freeze-thaw cycles mechanism. The second property that must be noted is the substantial uniformity of dates within the two separate groups of signs. The chronologies were collected around the 1000 a.C. for the billhooks and about three centuries later for the crosses, at least for the annual rain fall of 2150 mm/year, therefore clearly indicating the medieval origin of the artefacts.

However the dates concentration for the two groups does not necessarily imply that the signs were engraved in the same time because of the uncertainty of the single date values (shown by the vertical segment in each point of the Figure 10) and corresponding to about a century. This approximation is practically the amount of the random error caused by the joined effect of the granular stochastic erosive phenomena and of the differences in the shape of the moat in the various cross-sections of the engraving.

Finally it must be well noted the strong difference of dates between the group of the billhooks and the crosses, also neglecting the data related to 1750 mm/year annual rain fall in which it is very high. This difference, being well higher than the uncertainty due to the random error, seems to be due just to an historical or cultural reason rather than to a numerical one.

## CONCLUSIONS

In the present work, a method for absolute dating of rock art based on mathematical simulations and careful in situ experimental measurement has been proposed and presented. Beside the uncertainty of the input data required by the mathematical analysis, we believe that the exposed method is very promising for obtaining reliable absolute dates for rock art, at least and at present under the above described conditions which are limestone rocks, horizontal flat surfaces, open air exposure and figures traced in contour.

Note that, at least to our knowledge, the present proposal is the first example of rock art absolute dating using a specific technique for these artefacts. Other attempts reported in literature [Bednarick, R. G. 1979] [Dewdney, S. 1970] are generally based on reliable and well tested methods, as radiocarbon dating for the pigments of the paintings, radioactive isotopes or rock surface natural coating analysis, which were specially designed for other types of archaeological situations and whose results, in the case of rock art, may be easily polluted by materials coming from the rock substrate and hence may be largely unreliable.

The reported first experimental application of the dating method yielded results which are completely in agreement with our previous attempt of cultural interpretation of the rock art site [Bagnoli, P.E., Panicucci, N., Viegi, M., 2005], both from the chronological point of view between the Early Middle Age and the beginning of Middle Age and also from the point of view of the later dating of the crosses with respect to the billhooks, which strongly suggest the "Christianizing" procedure of pagan rocks used, or retained to be used, by pagan people for their rituals. This procedure typically occurred just in the first centuries of the Middle Age.

Beside we have well in mind that the data obtained for the Billhook Step may be still affected by a systematic error due to the uncertainties concerning some input parameters as the average annual rain fall, however we believe that the obtained chronological analysis of the engravings is substantially consistent and useful to demonstrate the validity of the proposed dating method. This implies that those interpretations of the billhooks locating them on one hand in the modern age (XIX century) and in the Etruscan or Roman period on the other one, including the ritual connection with the Silvanus god, can be discarded as completely wrong.

Further research developments concerning the present dating method proposal may involve suitable validation activities, i.e. the application on other rock art sites whose chronology may be obtained with certainty by an alternative method. Other future improvement of the method may include a refinement of the annual rain fall data by investigating the results of geological researches in the Apuane Alps, a modification of the simulation procedure in order to include in any way also the long-time fluctuations of the annual rain fall and the possible use of more sophisticated techniques for measuring the engraved profile such as laser interferometry.

## REFERENCES

- Bagnoli, P.E., Panicucci, N., Viegi, M., 2005, *Manifestazioni di arte rupestre figurativa sulle Alpi Apuane Centrali*, Atti del convegno ANTE ET POST LUNAM II - l'Evo Medio, Marina di Carrara, pp. 105-116.
- Citton, G., Pastorelli, I., 1995, *Incisioni rupestri sulle Alpi Apuane in alta Versilia*, Marsarosa, Lucca.
- Citton, G., Pastorelli, I., 2001, *I monti "scritti"*, Viareggio, Lucca.
- Sani G., 2006, *Le incisioni rupestri dei Pennati sulle Alpi Apuane e il culto del dio Silvano*, <http://www.simbolisullarocchia.it/archivio/lelamepennate/Lelamepennate.pdf>
- Guidi O., 1992, *Incisioni rupestri della Garfagnana*, Lucca.
- Szunyogh, G. 2005. *Theoretical investigation of the duration of karstic denudation on bare, sloping limestone surface*, Acta Carsologica 34/1 (1): 9-23.
- Buhmann D., Dreybrodt W. 1985. *The kinetics of calcite dissolution and precipitation in geologically relevant situations of karst areas. 1. Open system*, Chem. Geol. 48: 189-211.
- Svensson U., Dreybrodt W. 1992. *Dissolution kinetics of natural calcite minerals in CO<sub>2</sub>-water systems approaching calcite equilibrium*, Chem. Geol. 100: 129-145.
- Bednarick, R. G. 1979. *The potential of rock patination analysis in Australian archaeology - part 1*. The Artefact 4: 14-38.
- Dewdney, S. 1970. *Dating rock art in the Canadian Shield Region*. Occasional Paper 24, Art and Archaeology Series, Royal Ontario Museum, Toronto.



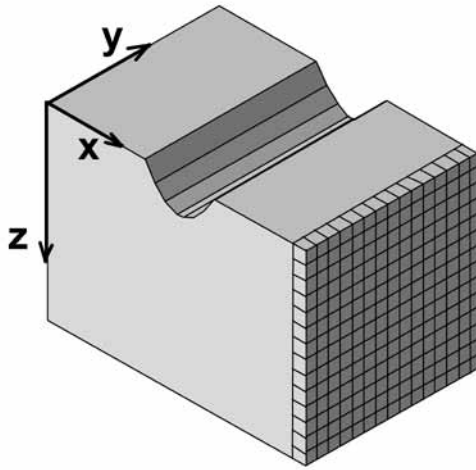


FIG. 1: View of the solid used for the simulations and its coordinate system.

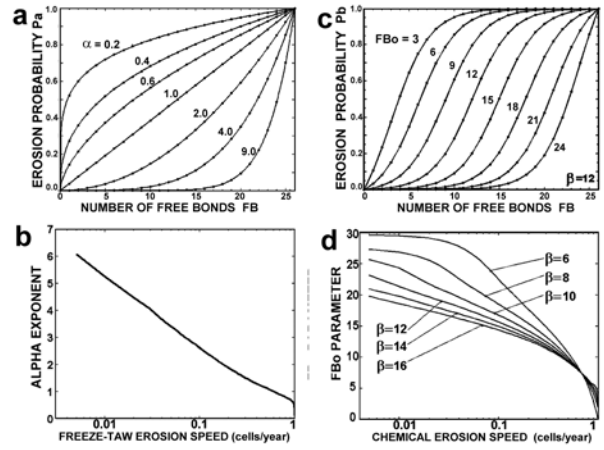


FIG. 2: a) Plots of the  $P_a$  probability functions vs. the number of free boundaries  $FB$  and for several  $\alpha$  values. b) Freeze-thaw erosion speed vs. the  $\alpha$  exponent. c) Plots of the  $P_b$  probability functions vs. the number of free boundaries  $FB$  and for several  $FBo$  values. d) Chemical erosion speed curves vs.  $FBo$  parameter.

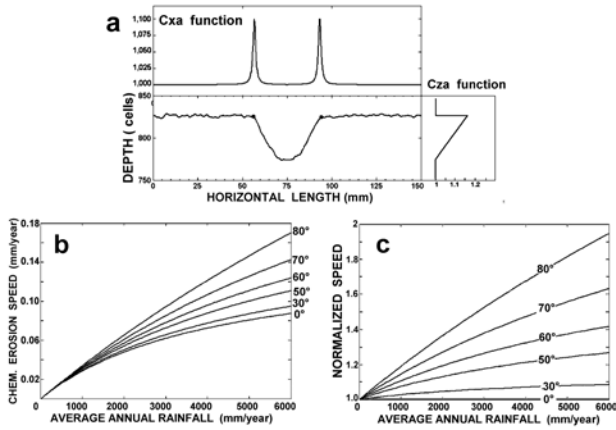


FIG. 3: a) Horizontal and vertical correction functions  $C_{xa}$  and  $C_{za}$  for the freeze-thaw erosion mechanism. b) Absolute and c) normalized chemical dissolution speed as functions of the annual rain fall for several values of the surface angle with respect to the horizontal plane.

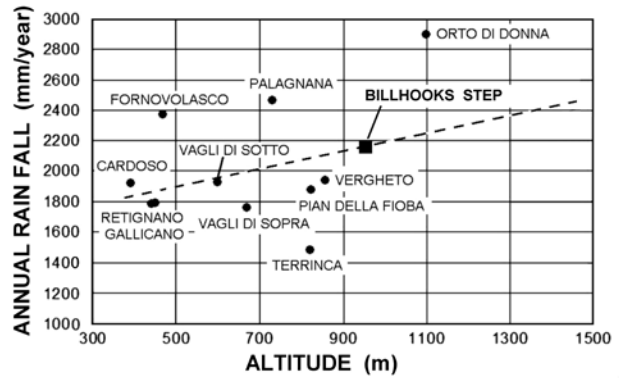


FIG. 4: Annual rain fall data from the measurement stations of the Apuane Alps as a function of the altitude.

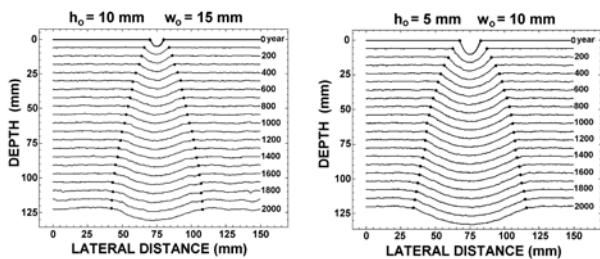


FIG. 5: Two simulations of the evolution of engraving profiles plotted in isometric scales and every 100 years.

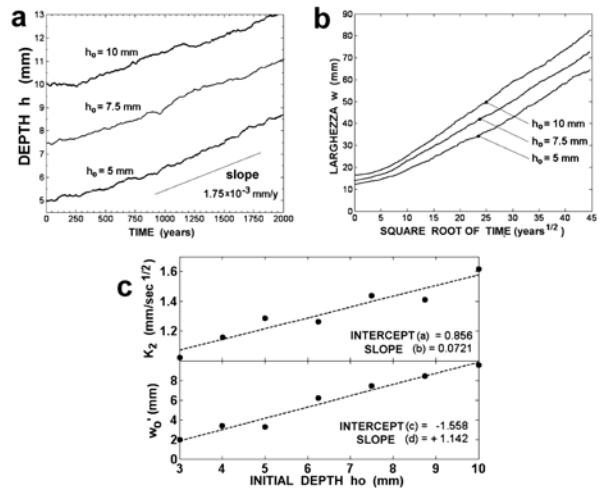


FIG. 6: Plots of the engraving depth (a) and width (b) vs. time and square root of time for three values of the initial depth  $h_0$ . c) Fitting plots for the calculations of the parameters  $a$ ,  $b$ ,  $c$  and  $d$  in the equations (11b).

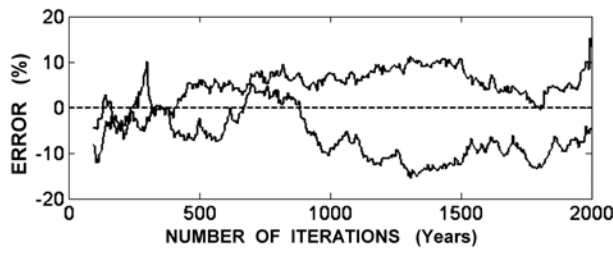


FIG. 7: Error percentage between the estimated time and the real one applied to the simulation results shown in the Figure 5.

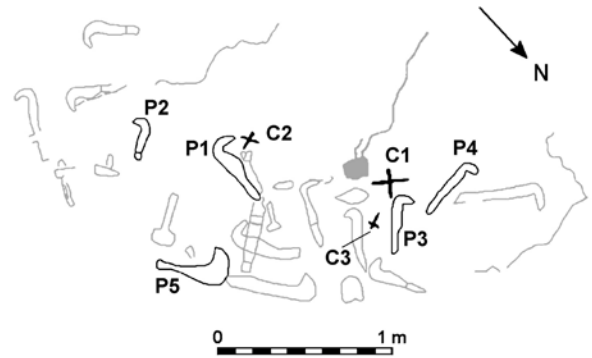


FIG. 8: Map of the engravings on the Billhooks Step (mount Gabberi, Camaione). The figure used for the dating experiment are drawn in black and labelled.

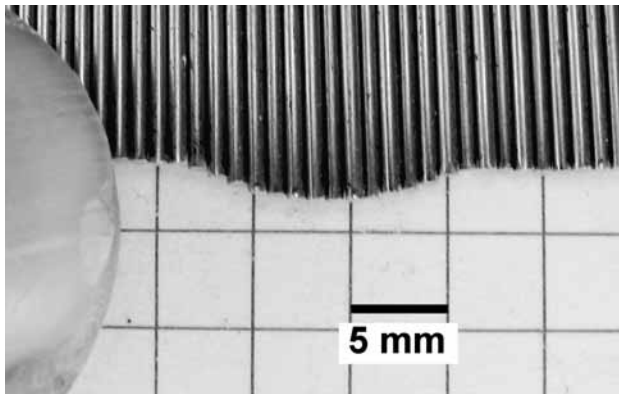


FIG. 9 : High resolution digital photograph used for the experimental measurement of the depth and width of an engraved figure.

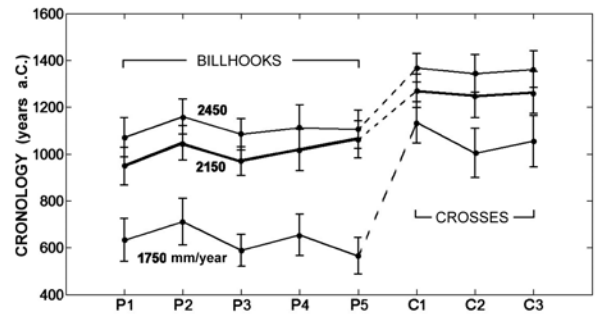


FIG. 10 : Plot of the chronologies of the eight figures for three different values of the average annual rain fall. The standard deviation for each date is also indicated by the vertical segments.

RAIN FALL	1750 (mm/year)			2150 (mm/year)			2450 (mm/year)		
	YEARS	DEV. (years)	DATE (y. a.C.)	YEARS	DEV. (years)	DATE (y. a.C.)	YEARS	DEV. (years)	DATE (y. a.C.)
P1 Billhook	1373	92	633	1058	81	948	935	83	1071
P2 Billhook	1295	99	711	959	74	1047	847	75	1159
P3 Billhook	1417	67	589	1036	61	970	922	66	1084
P4 Billhook	1351	88	655	989	88	1017	893	97	1113
P5 Billhook	1441	78	565	943	79	1063	901	81	1105
C1 cross	872	88	1134	736	71	1270	638	61	1368
C2 cross	1002	105	1004	758	92	1248	662	81	1344
C3 cross	951	110	1055	744	89	1262	644	78	1362

Table 1 : Numerical data for the chronologies of the eight figures for three different values of the average annual rain fall.